Electro-Synthesized Bismuth Oxide Nanomaterials on Flexible Substrate Electrode forSupercapacitor Application

V. B. Suryawanshi[1], R. G.Bobade[2],B. J. Lokhande[3], R. C.Ambare[2,*]

[1]Department of Chemistry, KMC, College, Khopoli, Khopoli-410203 (Affiliated to University of Mumbai), M.S. India.

[2]Department of Physics, KMC, College, Khopoli, Khopoli-410203 (Affiliated to University of Mumbai), M.S. India.

[3]Lab of Electrochemical Studies, School of Physical Sciences, PSAH Solapur University, Solapur, Maharashtra, India.

Abstract

The present article report on synthesis and electrochemical supercapacitor application of bismuth oxide (Bi_2O_3) deposited on stainless still (SS) substrate using alow cost and simplest electrodeposition methods. The structural analyses of the produced samples reveal polycrystalline with a tetragonal crystal structure. It has been obtained to synthesized linked adherence and compact surface morphologyand TEM reveals nanoplates-like surface appearance. Electrochemical supercapacitive concert of Bi_2O_3 thin film electrode has been performed through cyclic voltammetry (CV), charge-discharge (CD), and impedance spectroscopy (EIS) in aqueous 1M KOH electrolyte. The Bi_2O_3 thin film electrode obtained the highest specific capacitance (SC) of 1227.5 F/g at 2 mV/Sec scan rate in 1M KOH. Obtained maximum value of specific energy (SE) and specific power (SP) was 191.14 Wh/Kg and 4.8 kW/kg at 18 mA/cm^2 in 1M KOH electrolyte respectively. 93.29 % capacitance retention after 3500 CV cycles

Keywords: Bi_2O_3;Cyclic Voltammetry; Electrodeposition; Supercapacitor; Thin Films.

*Corresponding author: Dr. R.C. Ambare, E-mail address: revanambare@gmail.com, bjlokhande@yahoo.com.

1. Introduction

Supercapacitors, which are low-cost and ecologically benign energy storage alternatives, are developing demands in today's technology world. With unique pseudocapacitive charge storage processes, several transition metal oxides, such as RuOx, SnO_2, NiOx, MnO_2, IrOx, TiO_2, Co_3O_4, and Bi_2O_3, have been demonstrated to be effective electrode materials [1].The utilization of RuO_2 has the most success, although it is limited because of its expensive cost and scarcity. As a result, renewable, nontoxic, low-price, and non-noble metal oxides for supercapacitor electrodes are required. Bismuth oxide is a reduced hazardous transition metal oxide that has piqued the interest of researchers due to its broadband gap, photoconductivity, dielectric permittivity, high oxide ionic conductivity, and high refractive index [2].Lately, there has been a lot of interest in creating the cathode material for an electrolytic supercapacitor using nano crystallographic bismuth oxides. Nanocrystalline and highly distributed materials have a large surface area and a low diffusion route length for ions that can contribute significantly to supercapacitor performance development [3].

Bi_2O_3electrodeshave been prepared by numerousmethods such as electrodeposition, Successive ionic layer adsorption and reaction (SILAR), spray pyrolysis [4], atomic layer deposition, and chemical bath deposition (CBD). A few reports have occurred for the Bi_2O_3 as a supercapacitor thin film electrode. Gujar *et al.* have createda Bi_2O_3electrode via the ED method and describedthehighest SC of 98 F/g [5]. Ambare *et al.* have successfully synthesized Bi_2O_3 via the spry pyrolysis method and reported the obtained highest SC of 322.5 F/g at 5 mV/Sec in 1M Na_2SO_4 [4]. Zheng *et al.* created hierarchical rippling electrochemically synthesized Bi_2O_3 Nano belt electrodes having an optimum SC of 250 F/g and outstanding electrochemical durability [6]. Wang *et al.* reported graphene nanosheets and

Bi_2O_3composite electrode created via a simplistic solvothermal techniqueshowsoutstanding rate ability and glowing recycling stability with the SC of 757 F/g at 10 A/g [7].

The current study focused on the electrodeposition (ED) approach for generating Bi_2O_3 thin films from an aqueous solution being a potential technology due to its simplification, low price, and lack of sophisticated equipment. X-ray Diffraction (XRD) and field emission scanning electron Microscopy were used to characterize the acquired film (FE-SEM). Electrochemical investigations such as CV, CD, and EIS have also focused on using Bi_2O_3 thin film cathode electrodes for supercapacitor applications.

2. Experimental

2.1. Materials

All of the contaminants and solvents employed in this study, such as nitric acid and bismuth nitrate (S.D. Fine-Chem. Ltd.), were used without further purification. Before thin film deposition, a stainless-steel substrate (grade 46) was acquired locally, highly polished using zero-grade polish paper, and rinsed in an ultrasonic bath with double-distilled water (DDW) for 15 minutes.

2.2 Electrodeposition of Bi_2O_3

Double-distilled water was used to create consistent quantities of (0.1 M) $Bi(NO_3)_3$ (S.D. Fine-Chem. Ltd.). High-grade stainless steel (SS) (grade 46) substrate with 99% purity (1.5×5 cm^2) were selected as substrates. Substrates were subsequently polished using fine-grade polish paper before being etched in 10% H_2SO_4 for 20 seconds. Lastly, before deposition, they were ultrasonically washed in DDW. Bi_2O_3 depositions were performed for 15 minutes at a constant voltage of 1.6 V to develop functioning electrodes. Electrodes constructed at consistent concentrations were labelled as ED1 (0.1M) [8]. On the stainless stile (SS) substrate, a white bismuth hydroxide layer was produced. The obtained thin film

was annealed at 573 K for 60 minutes before being employed for structural, morphological, and electrochemical investigations.

2.3 Characterization details

Structural analysis of Bi_2O_3 thin film electrodes was made using an XRD Rigaku D/max 2550Vb, Cu-kα in the range of diffraction angle 2θ from 10^0 to 100^0. The surface morphology of the thin film was investigated by using anFE-SEM: Hitachi S 4800. A wettability study was made using a Holmark contact angle meter. TEM: Manufactured Hitachi (H-7650) Electron source-LaB6, Accelerating voltage- 80 ~ 120 kV, Point resolution (nm)-0.36, Line resolution (nm): 0.24, Magnification - HC mode - x200 ~ x200,000, HR mode – x 4,000 ~ x600,000, Field rotation: $\pm 90^0$ (15^0 step) for a magnification range of x1,000 to x40,000.The electrochemical studies were made using a computer-controlled potentiostat HCH 600D SPL electrochemical analyzer/workstation with standard three electrodes.

3. Results and Discussion

3.1 Film formation reaction kinetics

Electrolysis of $Bi(NO_3)_3$ in DDW. $Bi(NO_3)_3$ salt solution was prepared in DDW.

Possible Ionizations:

$$Bi(NO_3)_3 \rightarrow Bi^{3+} + 3NO_3^-$$

$$H_2O \rightarrow 2H^+ + O^{2-}$$

$$H_2O \rightarrow H^+ + OH^-$$

In an aqueous electrolytic reaction, H_2 was produced at the cathode and O_2 was produced at the anode as the NO_3^-, N is in the highest possible oxidation state (+5).

$$N^0 = 1s^1\ 2s^2\ 2p^3$$

$$N^{5+} = 1S^2\ 2S^0\ 2P^0$$

Possible Mechanism:

$$Bi(NO_3)_{3(s)} + 5H_2O_{(aq)} \rightarrow Bi(OH)_3\downarrow + 2H_2\uparrow + O_2\uparrow + 3HNO_{3(aq)}$$

Calcination reaction of obtained thin film

$$2\ Bi(OH)_3 \xrightarrow{573k} Bi_2O_3 + 3H_2O\uparrow$$

So obtained electrode of Bi_2O_3 was extremely steady against chemical humidity and corrosion.

3.2 Structural analysis

To examine the structural estimation of thin film electrode, XRD was scrutinized as shown in Fig.1. The diffraction peaks at 27.95^0, 32.73^0, 45.16^0, 46.28^0, 48.46^0, 54.30^0, 55.51^0, 59.68^0, 62.17^0, 68.54^0, 70.91^0, and 74.54^0 correspond to the (221), (400), (511), (402), (003), (223), (621), (403), (551), (800), (820) and (623) planes of tetragonal Bi_2O_3 (JCPDS 29-0236). Moreover, SS peaks are attributed to the stainless-steel substrate's distinctive peaks. The intensity and width of their distinctive XRD patterns were used to determine the crystallinity of Bi_2O_3 thin films. This is reliable with the findings of Raut *et al.* [9]. The average crystallite size of Bi_2O_3 was discovered to be ~33.38 nm.

3.3 Surface morphological and TEM analysis

FE-SEM images were used to investigate the surface morphology of as-deposited Bi_2O_3 films on SS at various magnifications. Fig.2(a-b) shows FE-SEM images of ED1 electrodes at different magnifications shows several well-dispersed nanomaterials on the SS substrate. It shows adherence and compact morphology. The resultant porous network of linked nanomaterials increases the volume of electroactive establishes for electrochemical reactions and shrinks the ion transportation route, leading to a greater kinetic for electrochemical processes [10]. Fig.2(c) Displays the contact angle of bismuth oxide (Bi_2O_3) thin films placed on stainless steel substrates. The contact angle demonstrates the hydrophilic nature of the material. The contact angle is determined by the material's surface shape and chemical composition. The thin yellow layer was scraped out and appropriately disseminated

in alcohol by resilient ultrasonic treatment before TEM evaluation since the Bi_2O_3 nanoplates were synthesized on the FTOsubstrate. Although some nanosheets were interconnected, as illustrated in Fig.3(a & b) similar results reported by Wang *et al* [11], the nanocrystals were almost homogeneous. Nanoplates typically have a diameter of ~ 29.87 nm.

3.4 Supercapacitive performance

CV was utilized to investigate the electrochemical properties of a Bi_2O_3 cathode electrode. The CV of a Bi_2O_3 film electrode in aqueous 1.0 M KOH was investigated in the voltage range of -1.0 to 0.7 V at varied scan rates ranging from 2 to 100 mV/s, as shown in Fig. 4(a). In 1.0 M KOH, the impact of scan rate on electrodeposited bismuth oxide was investigated throughout a voltage range of 2 to 100 mV. The current under the curve gradually grows as the scan rate rises. This demonstrates because the voltammetric currents are precisely proportional to the scan rate, indicating optimal capacitive performance [12]. Fig.4(b) depicts the fluctuation of individual capacitances with scan rate. As this scan rate is raised from 2 to 100 mV/Sec, the specific capacitances fall from 1227.5 F/g to 80.34 F/g. At 2 mV/Sec, the highest SC obtained was 1227.5 F/g. The greatest specific capacity reached in this investigation is greater than that stated in the literature, as shown in Table 1.The potential window and current density also expand with increasing scan rate, and curves begin to drift towards a positive potential end. Because Bi_2O_3 supports the higher scan rate for increased redox activity, the oxidation-reduction peaks demonstrate enhancement for higher scan rates. It can be challenging to continue the redox transition at higher scan rates because the charge and mass transfer resistance of material species diminishes due to IR drop [4]. The reduction in capacitance has been linked to the existence of innermost active sites, which are unable to completely maintain the redox transitions at greater scan rates. This is most likely owing to the proton's diffusion action within the electrode [13]. The declining trajectory of capacitance shows that at significant charging-discharging rates, sections of the electrode's surface are

impenetrable. As a result, the SC attained at the lowest scan rate is thought to be nearest to that of complete electrode material use. The redox peaks are due to the oxidation and reduction reactions takes place in the material. The reduction and the oxidation peak potential appeared in KOH electrolyte was similar to the reported Bi_2O_3 in hydroxide electrolyte [14]. The all CV curves shows the mixed capacitive behaviours. The detailed mechanism behind the oxidation and reduction process is described by Nithya *et al*. [14] for Bi_2O_3. During the reduction process, the following reaction takes place,

$$BiO_2^- \rightarrow BiO_{2\,(ads)}^-$$

$$BiO_{2\,(ads)}^- + e^- \rightarrow BiO_{2\,(ads)}^{2-}$$

$$3BiO_2^{2-} + 2H_2O \xleftrightarrow{Disproportionation} 2BiO_2^- + 4OH^- + Bi^0$$

$$Bi^{(0)} \rightarrow Bi_{(metal\,)}$$

During oxidation process, the following reaction takes place

$$Bi_{(metal\,)} \rightarrow Bi^+ + e^-$$

$$2Bi^+ \xleftrightarrow{Disproportionation} Bi^{3+} + 2Bi_{(metal\,)}$$

$$3OH^- + Bi^{3+} \rightarrow Bi\,(OH)_3$$

$$Bi\,(OH)_3 \rightarrow BiOOH + H_2O$$

Fig. 4. (c) Depicts the CD behavior of a Bi_2O_3 thin film electrode. CD behavior is not perfectly triangular for varied current densities of 18, 22, and 25 mA/cm^2, indicating the participation of the redox reaction mechanism in the Bi_2O_3 cathode electrode. The discharge profile typically consists of two parts: a resistive factor (linear section parallel to the y-axis) reflecting the voltage change attributable to internal resistance and a capacitive component (curved portion) indicating the voltage variation owing to energy shift within the capacitor [15]. CD technique were with increase in current density, charge-discharge time decreases,

showing inclination towards linear behavior.Additionally, the optimum SE and SP attributed to materials were estimated at approximately 191.14 Wh/kg and 4.8 kW/kg at 18 mA/cm^2 correspondingly. Fig. 4. (d) Depicts the change in energy and power with an appropriate current for the ED1 electrode.The CD curve causes a reduction in potential drop (ohmic drop), indicating the participation of pseudocapacitive behaviour. All CD curves exhibit IR drop, and the charging curve first increases before declining with extended plateaus. This is the beauty of Bi_2O_3, as proven by the fact that its discharge signatures differ from those of other materials. The polarisation effect may be affected by irreversibility in a system [4].

The stability curve results reveal that electrodeposition was used to create an extremely durable material. The system can tolerate over 3500 cycles without substantial capacity loss. This indicates the material is appropriate for energy purposes. The specific capacitance (SC) decreases only a little with cycling, as seen in Fig.4(e). According to this data, the specific capacitance of all electrodes decreases rapidly during the first 500 cycles but then remains nearly constant (until 3500 cycles). 93.29 % capacitance retention after 3500 CV cycles. Throughout the initial charge-discharge cycles, the active material may be lost due to disintegration and separation [16].

The electrochemical impedance of an annealed ED1 cathode was measured. The Nyquist graph with real and imaginary impedance values, the frequency range from 1 Hz to 1 MHz, measured at -0.60453 V open circuit potential (OCP), is shown in Fig.5. (a) The boundary point of the maximum frequency with an actual component of an impedance at high frequencies is the composition of electrolyte impedance, inherent substrate resistance, and contact resistance among the active material and the current collector. Interior resistance was around $\sim 0.81\ \Omega$. The significantly curved line structure with the gradient was diagnostic of ion diffusion into the thin film electrode materials in the intermediary frequency band. The continuous line component inclined additional towards the imaginary axis in the low-

frequency region, suggesting that the cathode electrode material had good capacitive performance [17, 18]. Fig.5(b) Depicts the Bode curve for the ED1 sample carried at 5 mA amplitude in 1M KOH. The graph shows that such phase angle increases with frequency, with capacitive nature dominating at knee frequency. The phase angle diminutions as frequency rise, demonstrating that resistance nature may predominance, i.e., at high-frequency entity material confirmed resistive existence and at lowest frequency domain material inveterate capacitive nature. Fig. 5(c) Displays the matched Nyquist plot of sample ED1 (Bi_2O_3) thin film electrode. The Nyquist plot for sample ED1 (Bi_2O_3) electrode attained via experiment and ordinary curves fit analyzed by ZsimpWin simulation software. The inset of Fig.5(c) Displays matched equivalent circuit for sample ED1 (Bi_2O_3) electrode having circuitry parameters viz charge transfer resistance R_1 = 0.9061 Ω, R_2 = 33.74 Ω, R_3 = 29.24 Ω, R_4 = 162.5 Ω, Q_1 = 0.0173 F, Q_2 = 0.0419 F, and C_1 = 0.0378 F.

4. Conclusions

The simple and minimal electrodeposition approach was used to effectively produce Bi_2O_3 thin film electrode. The tetragonal phase of the Bi_2O_3 thin film is shown by structural investigation. Interconnected adherence and compact morphology with nanoporous nature result in good electrochemical characteristics such as 1227.5 F/g specific capacitance with a good energy density of 191.14 Wh/kg ata power density of 4.8 kW/kg. Superior rate performance, 93.29 % retention after 3500 CV cycles. All of the abovementioned advantages demonstrate that our inventive strategy is promising in a wide range of nanoscale engineering.

Author's Contributions: V. B. Suryavanshi: Investigation and Validation, **R. G. Bobade:** Experimental synthesis, writing – original draft, Validation, Formal analysis, Software, and

Visualization. **B. J. Lokhande:** Supervision, Writing – review & editing draft. **R. C. Ambare:** Supervision, Writing – review & editing-original draft.

Funding: No funding.

Institutional Review Board Statement: Not applicable.

Informed Consent Statement: Not applicable.

Data Availability Statement: Data will be made available on request.

Conflicts of Interest: The authors declare that they have no known competing financial interests or personal relationships that could have appeared to influence the work reported in this paper.

Acknowledgments: Author Dr. R. C. Ambare expresses gratitude to Prof. (Dr.) B.J. Lokhande for supplying the electrochemical characterizations through financing projects of the Department of Science and Technology (DST), New Delhi, India, and the Bhabha Atomic Research Centre (BARC), Mumbai, for their monetary endorsement of the venture Policy 2010/34/46/BRNS/2228.

References

1. Kim H.K, Seong T.Y, Lim J.H., Cho W.L, Yoon Y.S. (2001). Electrochemical and structural properties of radio frequency sputtered cobalt oxide electrodes for thin-film supercapacitors. J. Power Sources, 102 (1-2), 167-171.
   DOI: https://doi.org/10.1016/S0378-7753(01)00864-3
2. Lee J-K., Pathan H. M., Jung K-D., Joo O-S. (2006). Electrochemical capacitance of nanocomposites films formed by loading carbon nanotubes with ruthenium oxide. J. of power sources, 159, 2, 1527-1531.
   DOI: https://doi.org/10.1016/j.jpowsour.2005.11.063
3. Pathan H.M., Sankapal B.R., Desai J.D., Lokhande C.D. (2003). Preparation and characterization of Nanocrystalline CdSe thin films deposited by SILAR method. Materials chemistry and physics, 78, 1, 11-14.
   DOI: https://doi.org/10.1016/S0254-0584(02)00198-0.

4. Ambare R.C., Shinde P., Nakate U.T., Lokhande B.J., Mane R. S. (2018). Sprayed bismuth oxide interconnected nanoplate supercapacitor electrode materials. Applied surface science. 453 214-219.
DOI: https://doi.org/10.1016/j.apsusc.2018.05.090

5. Gujar T.P., Shinde V.R., Lokhande C.D., Han S. (2006). Electrosynthesis of Bi2O3 thin films and their use in electrochemical supercapacitors. J Power Sources. 161, 1479- 1485.
DOI: https://doi.org/10.1016/j.jpowsour.2006.05.036

6. Zheng F., Li G., Ou Y., Wang Z., Su C., Tong Y. (2010). Synthesis of hierarchical rippled Bi2O3 nanobelts for supercapacitor applications. Chem. Commun. 46, 5021-5023.
DOI: https://doi.org/10.1039/C002126A

7. Wang H.W., Hu Z.A., Chang Y.Q., Chen Y.L., Lei Z.Q., Zhang Z.Y., Yang Y,Y. (2010). Facile solvothermal synthesis of a graphene nanosheets-bismuth oxide composite and its electrochemical characteristics. Electrochim Acta. 55 8974-8980.
DOI: https://doi.org/10.1016/j.electacta.2010.08.048

8. Lokhande B.J., Ambare R.C., Mane R.S., Bharadwaj S.R., (2013). Concentration-dependent electrochemical supercapacitive performance of Fe2O3. Current Applied Physics. 13, 6, 985-989.
DOI: https://doi.org/10.1016/j.cap.2013.01.04

9. Shrikant S.R., Omeshwari B., Babasaheb R. S. (2017). Synthesis of interconnected needle-like Bi2O3 using successive ionic layer adsorption and reaction towards supercapacitor application. Ionics. 23, 1831-1837.
DOI: https://doi.org/10.1007/s11581-017-1994-0

10. Bobade R.G., Nakate U.T., Roasiah P. Ouladsmane M., Lokhande B.J., Ambare R.C. (2023). Nanoarchitectonics of Bi_2CuO_4 electrodes for asymmetric Bi_2CuO_4//AC solid-state device in supercapacitor application. Inorganic chemistry communications, 154, 110998.
DOI: https://doi.org/10.1016/j.inoche.2023.110998

11. Wang, Y.; Jiang, L.; Tang, D.; Liu, F.; Lai, Y. (2015). Characterization of porous bismuth oxide (Bi_2O_3) nanoplates prepared by chemical bath deposition and post annealing. RSC Adv. 15, 65591-65594.
DOI: https://doi.org/10.1039/C5RA09949H

12. Hu C.C., Tsou T.W. (2002). Ideal capacitive behavior of hydrous manganese oxide prepared by anodic deposition. Commun. 4 (2), 105-109.
DOI: https://doi.org/10.1016/S1388-2481(01)00285-5

13. Chang K.H., Hu C.C. (2004). Oxidative synthesis of $RuOx.nH_2O$ with ideal capacitive characteristics for supercapacitors. J. Electrochem. Soc. 151, A958.
DOI: 10.1149/1.1755591

14. Nithya V.D., Sevan R.K., Kalpana D., Vasylechko L., Sanjeeviraja C. (2023). Synthesis of Bi_2WO_6 nanoparticles and its electrochemical properties in different electrolytes for supercapacitor electrodes. Electrochimica acta, 109, 720-731.
DOI: http://dx.doi.org/10.1016/j.electacta.2013.07.138.

15. Dubal D.P., Holze R., Romero G. (2014). Development of hybrid materials based on sponge supported reduced graphene oxide and transition metal hydroxides for hybrid energy storage devices. Sci. Rep. 4, 7349.
DOI: https://doi.org/10.1038/srep07349

16. Kotz R., Carlen M. (2000). Principles and applications of electrochemical capacitors. Electrochim. Acta. 45, 2483-2498.
DOI: https://doi.org/10.1016/S0013-4686(00)00354-6

17. Yana J., Wei T., Qiao W., Shao B., Zhao Q., Zhang L., Fan Z. (2010). Rapid microwave-assisted synthesis of graphene nanosheets/ Co3O4 composite for supercapacitors. Electrochim. Acta. 55, 6973-6978.
DOI: https://doi.org/10.1016/j.electacta.2010.06.081

18. Ambare R.C., Lokhande B.J. (2018). Spray pyrolysed Ni incorporated cobalt oxide thin film electrodes and their electrochemical study. J. of Mar. Sci: Mar. in Electronics. 29, 16289- 16294.
DOI:https://doi.org/10.1007/s10854-018-9718-4

19. Li, L.; Zhang, X.; Zhang, Z.; Zhang, M.; Cong, L.; Pan, Y.; Lin, S. (2016).A bismuth oxide nanosheets-coated electrospun carbon nanofiber film: a free-standing negative electrode for flexible asymmetric supercapacitors. J. Mater. Chem. A**,** 4, 16635-16644.
DOI: https://doi.org/10.1039/C6TA06755G

20. Xu,H.; Hu, X.; Yang, H.; Sun, Hu,Y.C.;Huang, Y. (2014).Flexible asymmetric micro-supercapacitors based on Bi_2O_3 and MnO_2 nanoflowers: larger areal promises higher energy density. Adv. Energy Mater, 5, 1401882.
DOI: https://doi.org/10.1002/aenm.201401882

21. PooladiM., ZerafatM. M. (2023). Three-dimensional flowerlike, two dimensional sheet-like, and one dimensional rod-like mesoporous Bi_2O_3 nanostructures for high performance asymmetric supercapacitors. Journal of physics chemistry of solid, 180, 111486.

DOI: https://doi.org/10.1016/j.jpcs.2023.111486

22. Han Y., Li L., Liu Y., Li X., Qi X., Song L. (2018) Fabrication of strontium bismuth oxide as novel battery-type electrode materials for high-performance supercapacitors.

DOI: https://doi.org/10.1155/2018/5078473

23. Ji Z., Dai W., Zhang S., Wang G., Shen X., Liu K., Zhu G., Kong L., Zhu J. (2020). Bismuth oxide/nitrogen-doped carbon dots hollow and porous hierarchitectures for high-performance asymmetric supercapacitors. Advance powder technology, 31, 2, 632-638.

DOI: https://doi.org/10.1016/j.apt.2019.11.018

Figure:

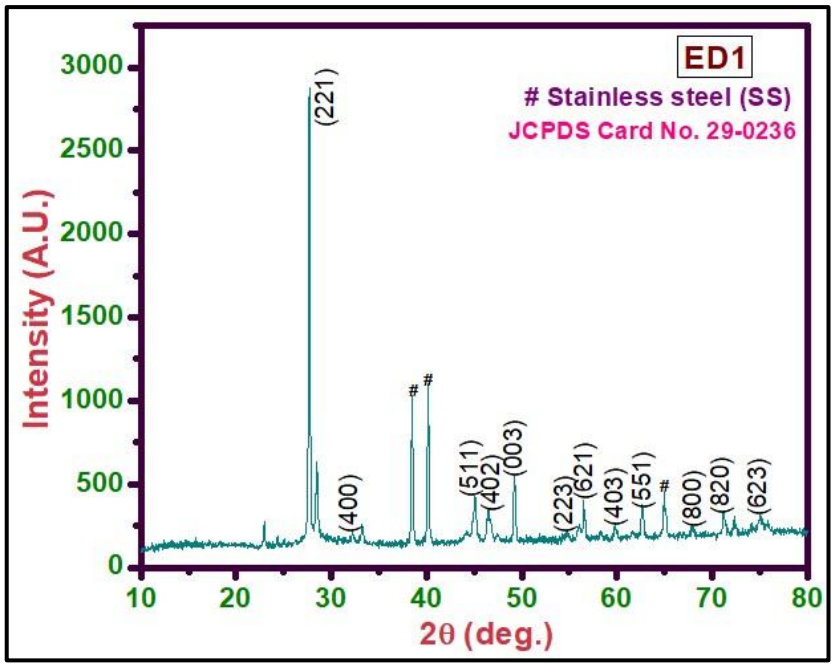

Fig. 1.XRD pattern of Bi_2O_3thin film on SS substrate.

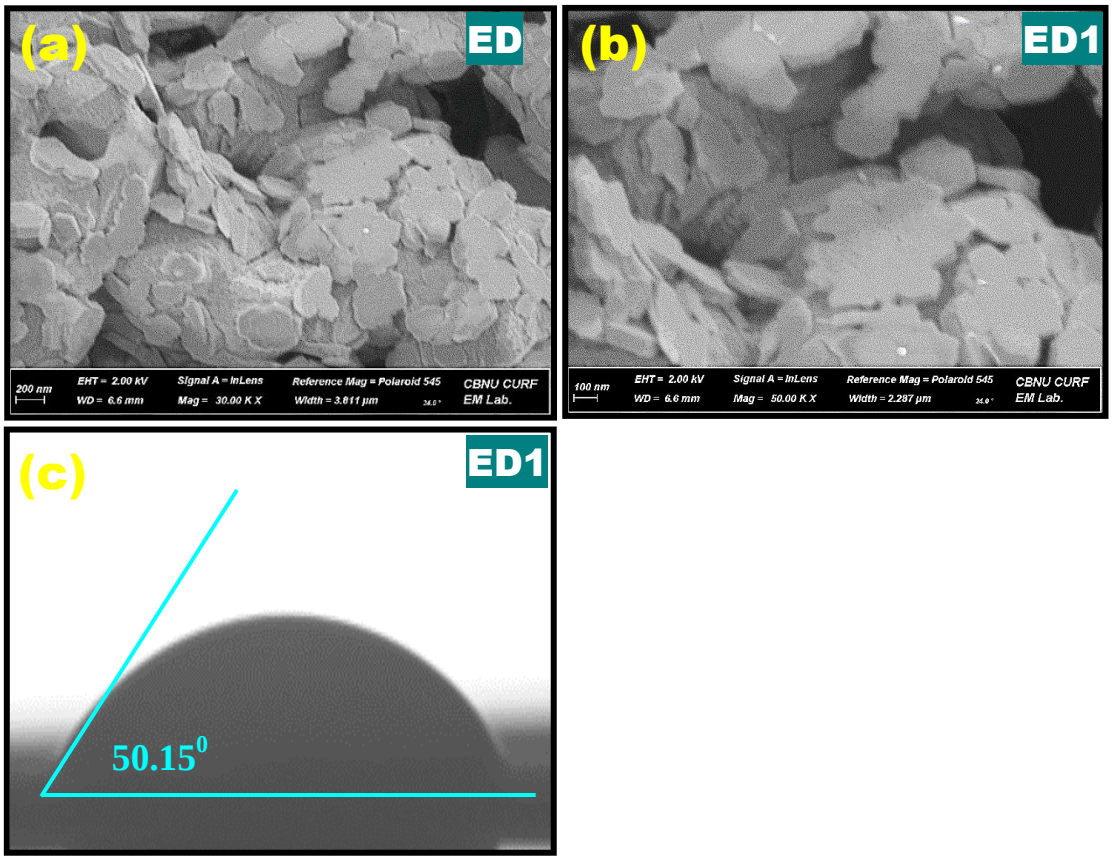

Fig. 2.(a), (b) FE-SEM images of the Bi_2O_3thin film (ED1) at two different magnifications.**c)**Wettability images of ED1, of Bi_2O_3 thin films deposited on SS substrates.

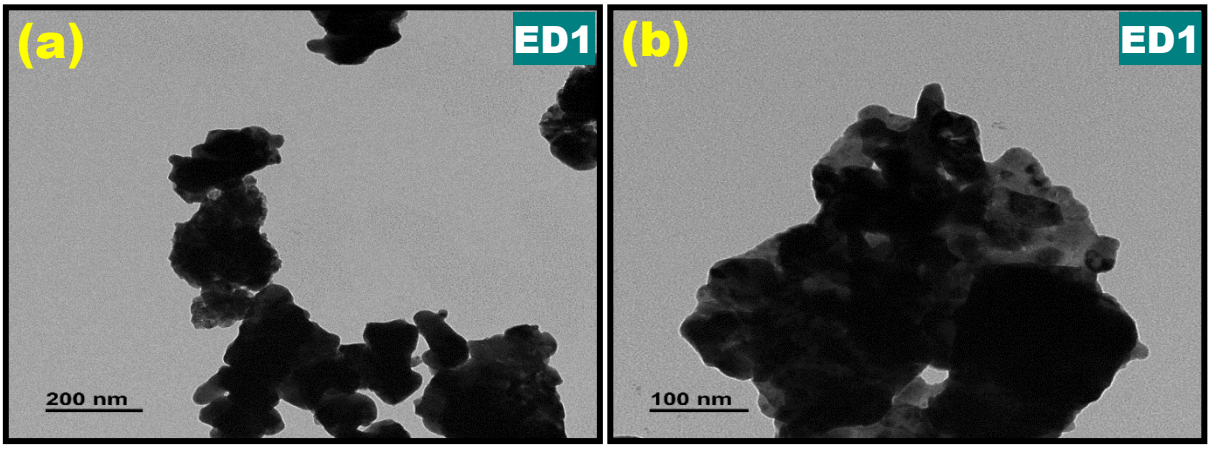

Fig. 3. TEM images of sample ED1 (Bi_2O_3) at (a) lower magnification 200nm, (b) higher magnification 100nm.

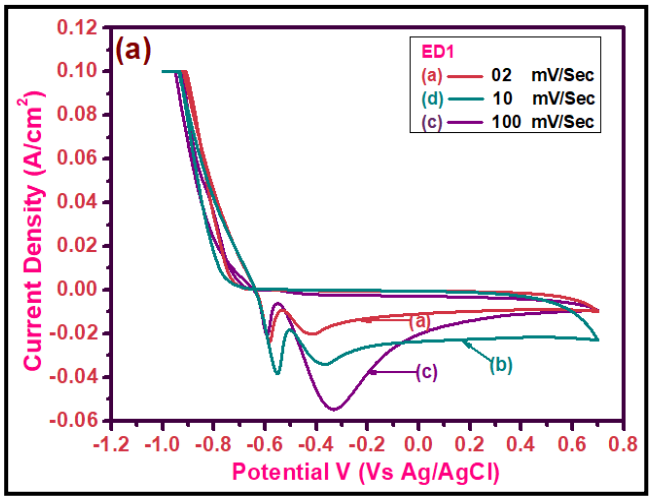
(a)
ED1
(a) 02 mV/Sec
(d) 10 mV/Sec
(c) 100 mV/Sec
Current Density (A/cm2)
Potential V (Vs Ag/AgCl)
(a)
(b)
(c)

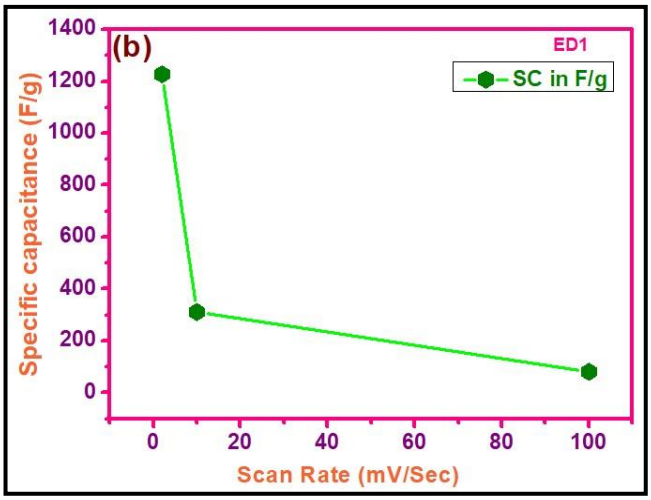
(b)
ED1
SC in F/g
Specific capacitance (F/g)
Scan Rate (mV/Sec)

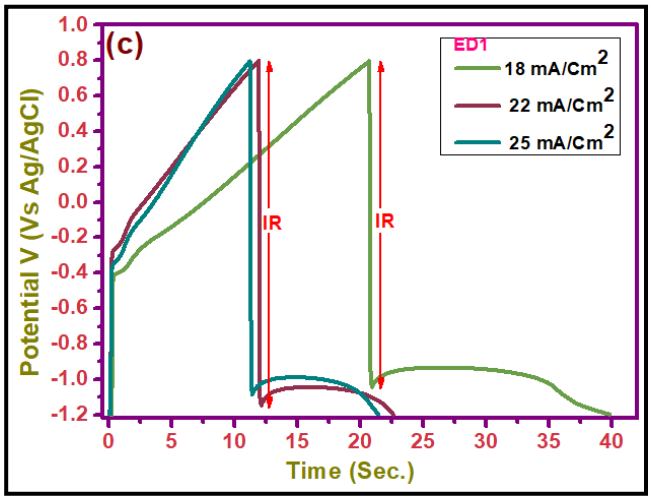
(c)
ED1
18 mA/Cm2
22 mA/Cm2
25 mA/Cm2
IR
IR
Potential V (Vs Ag/AgCl)
Time (Sec.)

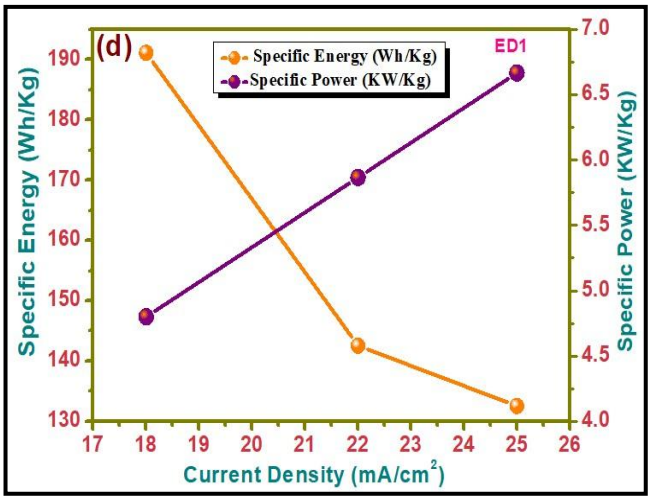
(d)
ED1
Specific Energy (Wh/Kg)
Specific Power (KW/Kg)
Specific Energy (Wh/Kg)
Specific Power (KW/Kg)
Current Density (mA/cm2)

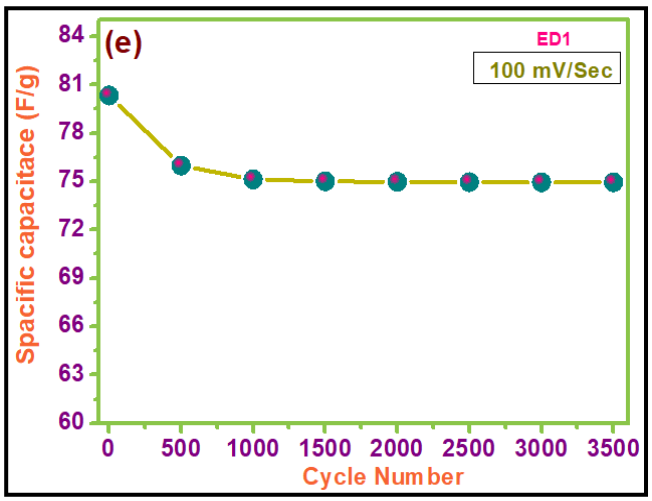
(e)
ED1
100 mV/Sec
Spacific capacitace (F/g)
Cycle Number

Fig. 4. (a) CV curves at different scan rate in 1M KOH electrolyte with potential windo (-1.0 to 0.7 V) Vs Ag/AgCl.(b) Variation of specific capacitance and scan rate of ED1 electrode in 1M KOH electrolyte.(c) Charge-discharge curve at different current densities in 1M KOH electrolyte. (d) Variation of energy and power with current density of ED1 electrode.(e) Variation of capacity retention with the number of cyclesat 100 mV/Sec scan rate of ED1 electrode.

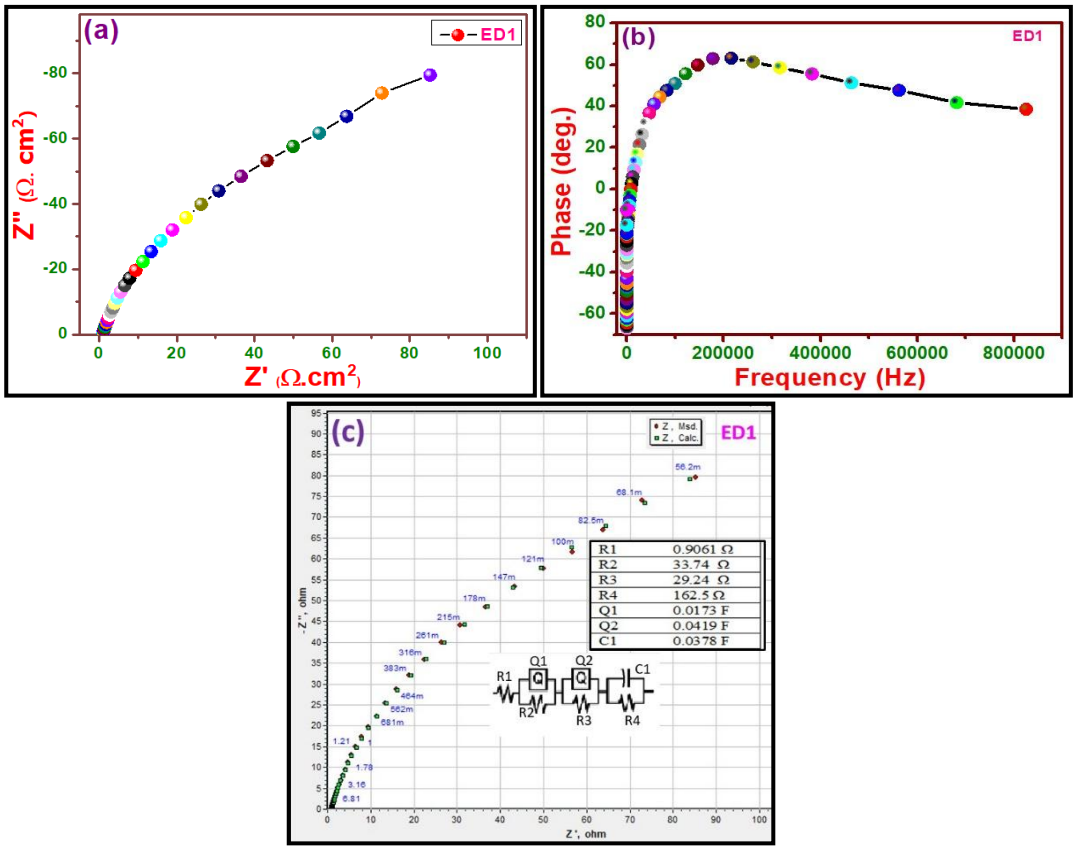

Fig.5. Sample (ED1) scanned in 1 M KOH impedance study(a) Nyquist plot (b) Bode plot, (c) matched Nyquist plot.

Table 1: The comparison of electrodeposited bismuth oxide on stainless steel substrate with other reported bismuth oxide electrode in aqueous electrolyte.

Working Electrode	**Synthesis Method**	**Electrolyte**	**Specific Capacitance (SC) in F/g**	**Stability**	**References**
Bi_2O_3	Spray Pyrolysis	1M Na_2SO_4	322.5	92% retention after 5000 cycles.	[4]
Bi_2O_3	Electrodeposition	1M NaOH	98	----------	[5]
Bi_2O_3/graphene	Solvothermal Method	6M KOH	757	65% retention after 1000 cycles.	[7]
Bi_2O_3	Electrospinning Technology	1M Na_2SO_4	786.2 mF/g	87% retention after 2000 cycles.	[19]
Bi_2O_3	Anodizing Method	1M Na_2SO_4	25.2	65% retention after 1000 cycles.	[20]
Bi_2O_3	Precipitation Method	6 M KOH	1350	94.9 % retention after 6000 cycles.	[21]
$Sr_2Bi_2O_5$	Impregnation-calcination method	6M KOH	1228.7	75.1 % retention after 3000 cycles.	[22]
Bismuth oxide/ carbon dots	Solvothermal method	3M KOH	1046	83.5 % retention after 1500 cycles.	[23]
Bi_2O_3	**Electrodeposition Method**	**1M KOH**	**1227.5**	**93.29 % retention after 3500 cycles.**	**In this work**

Graphical abstract